2007 IEEE International Conference on
Robotics and Automation
Roma, Italy, 10-14 April 2007

Passive Swing Assistive Exoskeletons for Motor-Incomplete Spinal Cord Injury Patients

Kalyan K Mankala, Sai K Banala and Sunil K Agrawal

Abstract— **In this paper, we present a passive device for swing assistance of motor-incomplete spinal cord injury patients. This device is aimed at reducing the physical demands on the therapists during treadmill training. We model the human leg as two links and a point foot mass, with a moving trunk. We employ passive elements in the design which get charged by the treadmill. Using the system dynamics, we optimize the design parameters to obtain a feasible swing motion of the leg. An exoskeleton was constructed based on these design parameters and tests were performed on a healthy subject at different treadmill speeds.**

I. Introduction

The incidence of spinal cord injury (SCI) in the United States is approximately 11,000 per year, with a prevalence of ≈250,000 [1]. Damage to the spinal cord often results in loss of ambulation. Approximately, 52% of this population have motor incomplete lesions [1] and, therefore, the potential to regain functional ambulation. Currently, therapist assisted body-weight supported treadmill training (BWSTT) is used for rehabilitation of SCI patients [2]. Various motorized (robotic) devices have been developed for rehabilitation of the lower limbs. For example, the Lokomat [3] is an exoskeletal orthosis, instrumented with bilateral hip and knee actuators, for locomotion training. Such motorized devices are expensive and long-term benefits from these are still under investigation [4]. Gottschall and Kram [5] proposed a simple, non-motorized devices which can apply adjustable forces to assist limb swing and forward propulsion during walking. Non-motorized devices have also been developed to assist upper extremity movements by eliminating or reducing the effects of gravity in individuals with arm impairments [6], and for the lower extremity to help in gait training [7], [8]. Such devices are relatively inexpensive and indicate that adjustable assistance to the lims is possible during training to maximize voluntary motor activity.

In this paper, we present a simple passive device for swing assistance of patients with iSCI and show simulation and experimental results. In order to scientifically design the swing assist bilateral orthosis, we used mathematical models to predict the natural motion of the leg, once it gets strapped to the orthosis. The model of the swinging leg provides insights into the motion and brings a framework for optimization of the parameters of the exoskeleton. Our design of the swing assistive exoskeleton consists of two torsion springs - one at the hip joint and the other at the knee joint whose torsion constants and equilibrium configurations form the design parameters. The organization of the rest of the paper is as follows: In Section II, we describe the dynamics of the human leg during swing and optimize the design parameters to obtain a feasible gait. In Section III, we discuss an exoskeleton design and test results on a healthy subject at different treadmill speeds. These are followed by conclusions of the work.

Kalyan K Mankala is a PostDoc in the Department of Mechanical Engineering, University of Delaware, Newark, DE 19716, USA mankala@ieee.org

Sai K Banala is a Graduate Student in the Department of Mechanical Engineering, University of Delaware, Newark, DE 19716, USA banala@udel.edu

Sunil K Agrawal is a Professor in the Department of Mechanical Engineering University of Delaware, Newark, DE 19716, USA agrawal@udel.edu

II. Model

Figure 1 shows the model of a human leg moving on a treadmill in the sagittal plane (X-Y plane). Leg is modeled as having two links - thigh, shank and two joints - hip and knee. The foot is considered as a point mass at the end of the leg. The swing assistance device consists of two torsion springs - one at the hip joint and the other at the knee joint. The stiffness constants c_1, c_2 and the equilibrium configurations $\theta_{1_{eq}}$, $\theta_{2_{eq}}$ of these springs are considered to be design parameters. The system dynamics depends on the following quantities: m_1, m_2 - masses of the thigh and shank; L_1, L_2 - lengths of thigh and shank segments; L_{c_1}, L_{c_2} - location of the center of mass of the thigh and shank measured from the respective joints; I_1, I_2 - inertia of thigh and shank about their center of mass. In this model, we

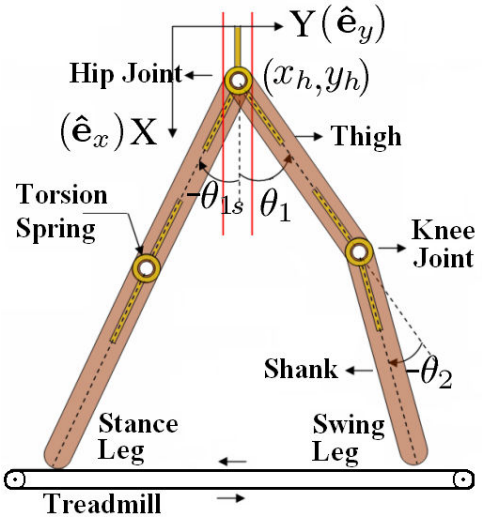

Fig. 1. Model of a human leg in the sagittal plane with hip moving as an inverted pendulum

assume that hip only has vertical motion, i.e., it is assumed to be inertially fixed in the horizontal direction. As the motion of hip and stance leg are related, using a kinematic model for the stance leg, we compute the motion of hip which is then used to find the dynamics of swing leg. In this kinematic model, we assume that the bottom (foot) of stance leg is in continuous contact with a treadmill and slides along with the treadmill until the swing leg makes contact again. We also assume that the knee is locked during the stance phase.

If the treadmill moves at a constant speed v, the position of the contact point of the stance leg with the treadmill, y_{ft}, at time t, is given as

$$y_{ft} = y_{ft_0} + vt, \tag{1}$$

where y_{ft_0} is the position of the contact point at the start of the stance phase. Let x_t be the position of treadmill in the $\hat{\mathbf{e}}_x$ direction. Using kinematics, we write the vertical position of the hip as

$$x_h(t) = x_t - \sqrt{(L_1+L_2)^2 - (vt + y_{ft0} - y_h)^2}, \tag{2}$$

$$y_h(t) = 0 \quad \text{(hip inertially fixed in horizontal direction).} \tag{3}$$

Hip angle during stance phase θ_{1s} is given as

$$\theta_{1s} = \tan^{-1}\left(\frac{y_{ft} - y_h}{x_t - x_h}\right). \tag{4}$$

A. Equations of Motion

Swing leg dynamics can be written using the Lagrange equations.

$$\frac{d}{dt}\frac{\partial \mathcal{L}}{\partial \dot{\theta}_i} - \frac{\partial \mathcal{L}}{\partial \theta_i} = 0, \qquad i = 1, 2. \tag{5}$$

The Lagrange function is defined as follows,

$$\mathcal{L} = K.E. - P.E. \tag{6}$$

where

$$K.E. = \frac{1}{2}m_1\dot{\mathbf{r}}_{1_{cm}}^2 + \frac{1}{2}I_1 w_1^2 + \frac{1}{2}m_2\dot{\mathbf{r}}_{2_{cm}}^2 + \frac{1}{2}I_2 w_2^2 \tag{7}$$

$$P.E. = -m_1 g(\mathbf{r}_{1_{cm}} \cdot \hat{\mathbf{e}}_x) + \frac{1}{2}c_1(\theta_1 - \theta_{1_{eq}})^2 - m_2 g(\mathbf{r}_{2_{cm}} \cdot \hat{\mathbf{e}}_x) + \frac{1}{2}c_2(\theta_2 - \theta_{2_{eq}})^2 \tag{8}$$

$$\mathbf{r}_{1_{cm}} = [x_h + L_{c_1}\cos(\theta_1)]\hat{\mathbf{e}}_x + [y_h + L_{c_1}\sin(\theta_1)]\hat{\mathbf{e}}_y \tag{9}$$

$$\mathbf{r}_{2_{cm}} = [x_h + L_1\cos(\theta_1) + L_{c_2}\cos(\theta_1+\theta_2)]\hat{\mathbf{e}}_x + [y_h + L_1\sin(\theta_1) + L_{c_2}\sin(\theta_1+\theta_2)]\hat{\mathbf{e}}_y \tag{10}$$

In the above equation, $\hat{\mathbf{e}}_x$ and $\hat{\mathbf{e}}_y$ are unit vectors along X and Y axes.

B. Knee Locking and Unlocking

In humans, the knee joint gets locked if the shank tries to move past $\theta_2 = 0$. This knee locking event is an instance of impact. Once we obtain optimized design parameters, during forward simulation of dynamics, we account for knee locking and unlocking events. The impact equations corresponding to knee locking event are obtained from the conservation of angular momentum about hip joint.

$$H^-_{O,leg} = m_1\left[\dot{y}_h\cos(\theta_1) - \dot{x}_h\right]L_{c_1} + m_1 L_{c_1}^2\dot{\theta}_1^- + I_1\dot{\theta}_1^- + m_2\left[\dot{y}_h(L_1+L_{c_2})\cos(\theta_1) - \dot{x}_h(L_1+L_{c_2})\sin(\theta_1)\right] + m_2(L_1+L_{c_2})\left[(L_1 + L_{c_2}\dot{\theta}_1^-) + L_{c_2}\dot{\theta}_2^-\right] + I_2(\dot{\theta}_1^- + \dot{\theta}_2^-) \tag{11}$$

$$H^+_{O,leg} = mL_c\left[\dot{y}_h\cos(\theta_1) - \dot{x}_h\sin(\theta_1)\right] + mL_c^2\dot{\theta}_1^+ + I\dot{\theta}_1^+ \tag{12}$$

In the above equations '+' superscript indicates quantities after impact and '-' indicates quantities before impact. $H_{O,leg}$ denotes the angular momentum of the leg about hip joint, $m = m_1 + m_2$, I denotes the moment of inertia of the whole leg about its center of mass. Equating the angular momentum before and after impact, we obtain $\dot{\theta}_1^+$ from the knowledge of θ_1, θ_2, $\dot{\theta}_1^-$ and $\dot{\theta}_2^-$.

Knee unlocking occurs when the reaction torque due to torsion spring, gravity force and shank acceleration is not positive. This condition is expressed in equation as follows

$$-m_2 g L_{c_2}\sin(\theta_1) + c_2\theta_{2_{eq}} - m_2 L_{c_2}\left(-\ddot{x}_h\sin(\theta_1) + \ddot{y}_h\cos(\theta_1) + (L_1 + L_{c_2}\ddot{\theta}_1)\right) \leq 0 \tag{13}$$

In general, knee unlocking does not occur until the swing leg touches the ground.

C. Design Optimization

The optimization of the design is schematically described in Fig. 2. Given the desired initial and final configurations of the swing leg, the design parameters $c_1, c_2, \theta_{1_{eq}}, \theta_{2_{eq}}$ are found from an optimization routine that gives a feasible gait. During optimization, while solving system dynamics, to prevent the knee angle from going above zero degree, we use an additional stiff spring that applies torque when the knee angle $\theta_2 > 0$. In the optimization, the error from the swing final configuration is minimized, while a positive ground clearance at a discrete number of points is imposed as a constraint. The optimized parameters are then used to perform forward simulations. During forward simulations, the additional stiff spring is not used but instead the knee locking and unlocking model is used.

D. Simulation Results

The following average anthropometric data for human leg [9], whose average body weight is 72.6 kg, is used to obtain the simulation results.

m_1	= 0.1000× BodyWt
m_2	= 0.0465× BodyWt
m_3	= 0.0145× BodyWt = foot mass
L_1	= 0.41 m
L_2	= 0.40 m
L_{c_1}	= 0.433× L_1
L_{c_2}	= 0.433× L_2
R_1	= 0.323× L_1 (radius of gyration of thigh)

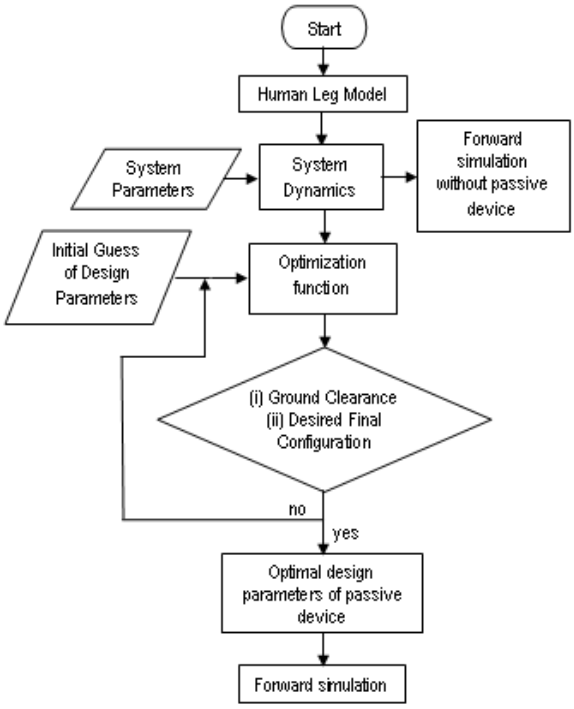

Fig. 2. The schematic of the optimization of the parameters of the swing assistive orthosis.

R_2 = 0.302× L_2 (radius of gyration of shank)

The initial configuration of the swing leg is taken as $[\theta_{10}, \dot{\theta}_{10}, \theta_{20}, \dot{\theta}_{20}] = [-\pi/6.022, \dot{\theta}_{1s}, 0, 0]$ and the final desired configuration as $[\theta_{1f}, \dot{\theta}_{1f}, \theta_{2f}, \dot{\theta}_{2f}] = [\pi/6.022, \dot{\theta}_{1s}, 0, 0]$. Desired gait time is chosen as 0.7 s. With these system parameters and desired configurations, the optimization routine gives the design parameters as $c_1 = 0.427$ Nm/rad, $c_2 = 11.337$ Nm/rad, $\theta_{1_{eq}} = 180^o$, $\theta_{2_{eq}} = -98.1^o$.

For the stance leg, we specify the symmetrically opposite initial conditions, i.e., the final configuration of swing leg is taken as the initial configuration of the stance leg and the initial configuration of the swing leg is taken as the final configuration of the stance leg. Speed of the treadmill is then calculated by specifying the desired time to take one step which we considered as 0.8 s. This would translate to a treadmill speed of 1.9 mph.

Apart from the thigh and shank mass, in this simulation, we also consider foot mass and device mass. We assume that the device mass for the thigh and shank segments is 1 kg each and is distributed such that their center of mass and radius of gyration coincide with center of mass and radius of gyration of thigh and shank segments repectively. One set of design parameters obtained from optimization routine are $c_1 = 7.90$ Nm/rad, $c_2 = 5.35$ Nm/rad, $\theta_{1_{eq}} = 22.2^o$, $\theta_{2_{eq}} = 0^o$. Using these optimized design parameters, we perform one step and multistep simulations. Figure 3 shows the stick diagrams of leg motion for one step simulation. The red dotted line shows the motion of stance leg and the blue solid line shows the motion of swing leg. The initial position of swing leg is shown by a thick blue line with diamond markers and the desired final position is shown by a brown line with star markers. Figure 3(i) shows the leg motion when the device is used with optimized design parameters - swing leg has good ground clearance and goes close to the desired final configuration. Figure 3(ii) shows the leg motion when the design parameters are kept constant but the leg mass is changed by 50% - even in this case swing leg reaches goal point in a desirable manner. The gait in these cases takes between 0.8 and 0.85 seconds to complete. These results show that the system is robust to variations in leg mass. For a multistep simulation, we use the configuration of leg from previous step as a initial configuration for the next step. These plots are shown in Fig. 4. From these plots, we observe that the joint trajectories are stable and also robust to changes in leg mass.

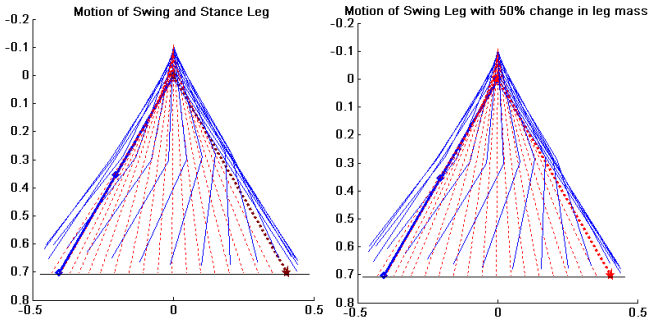

Fig. 3. Motion of stance leg and swing leg - (i) with assistive device and optimal parameters of the torsional spring; (ii) With assistive device and optimal parameters of the torsional spring but with 50% change in leg mass. Stance leg - red dotted line. Swing leg - blue solid line. Initial position of swing leg - thick blue line with diamond markers. Final position of swing leg - brown line with star makers.

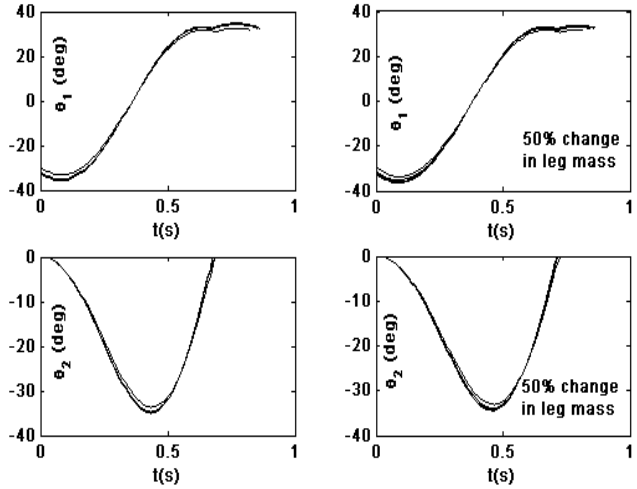

Fig. 4. Joint trajectories of swing leg for 100 step simulation with optimial parameters of torsion spring - (i)θ_1 vs time (ii) θ_2 vs time. With 50% change in leg mass - (iii)θ_1 vs time (iv) θ_2 vs time

E. Discussion

In a human, hip moves up and down during walking. Looking at the device from the energy flow point of view, we

see that the springs get charged during the stance phase with the help of treadmill and the body-weight support system. In swing phase, the potential energy stored in springs is converted to kinetic energy of the swing leg. Also, during this swing motion, some work is done at the hip - the boundary of swing leg and stance leg. So, energy flows in and out of the swing leg due to force interaction at the hip. Some amount of energy is lost in knee impact (knee locking event) and some energy is lost in heel-strike event (heel of the swing leg impacting with the treadmill at the end of swing phase) thus returning the energy level of leg back to its previous state. Heel strike event is not modeled in this paper as we look at only the kinematic model of the leg after the heelstrike and not its dynamic model. In human walking, there is a non-zero, finite-time double support phase. In this phase, both swing leg and stance leg are in contact with the ground. If we model the foot in our design, this double support phase should also be modeled.

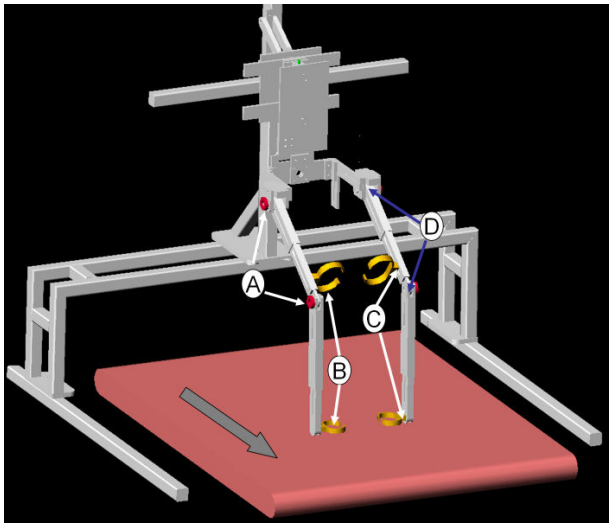

Fig. 5. AutoCAD drawing of Swing Assistance Device with Body Weight Support system and treadmill - (i) A. Torque Springs B. Straps C. Force Torque Sensors at robot human interface D. Encoders at the Joints.

III. Experimental setup and Results

Fig. 5 shows the AutoCAD drawing of an exoskeleton to experimentally verify the effects on human gait. This AutoCAD drawing provides an overview of its various components. Figure 6 shows the experimental set up of a healthy subject wearing the passive swing assistive device. The device consists of a trunk belt that is strapped onto the human trunk. A pelvis link made of aluminum is rigidly attached to the trunk belt. To help the pelvis link stay vertical, while the human walks on a treadmill, a back pack frame is used. The back pack frame is rigidly connected to the pelvis link through adjustable 80-20 aluminum sections. Other links present in the device are the thigh and shank links. All the links are connected successively through revolute joints. All links have slots in them to adjust the link lengths to that of the human wearing the device. This helps in matching the device joint axes with that of the human. The device thigh link is connected to the human thigh with the help of a thigh brace. The device shank link is connected to the human foot via a foot piece that is attached to the shank link. The foot piece currently does not allow ankle degree of freedom but it allows certain bending of human ankle. At the device hip and knee joints, torsion springs are connected parallely to obtain a desired stiffness and equilibrium configuration, suggested by the optimization. Encoders are placed at all revolute joints to measure hip and knee angles. Two force-torque sensors are present in the device, one sandwiched between the thigh link and the thigh brace and the other sandwiched between the shank link and the foot piece. These sensors measure the forces and torques transmitted between the device and the human.

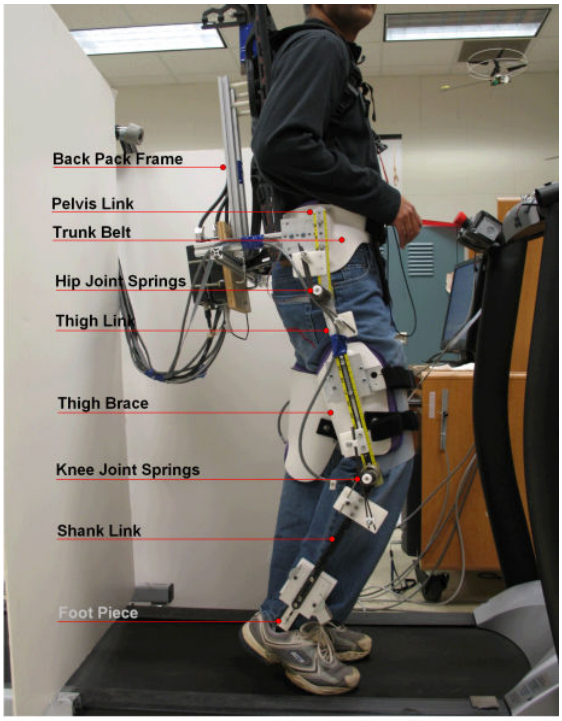

Fig. 6. Experimental set up - Healthy subject wearing passive swing assistive device.

Data was collected when a subject walked on a treadmill at different speeds. A 20 point moving average method was used to smoothen the joint encoder data. Joint velocities and acceleration were found using central difference scheme. Figure 7(a) shows the joint data, θ_2 vs θ_1, of a trial where the treadmill speed was 2 mph. Note that, in Sec. II, the optimized spring parameters correspond to 1.9 mph treadmill speed. Hence, we show the results of this trial in more detail. In this figure, different loops indicate different steps taken during a trial. Red lines represent swing phase, extracted from full step data represented by red and blue lines combined. Solid black line represents average swing phase. The same data is plotted against time in Figs. 7(b),(c).

To evaluate the effectiveness of the device, we analyzed the data using the following two cases. In case 1, we estimated the torque applied by the human when he is

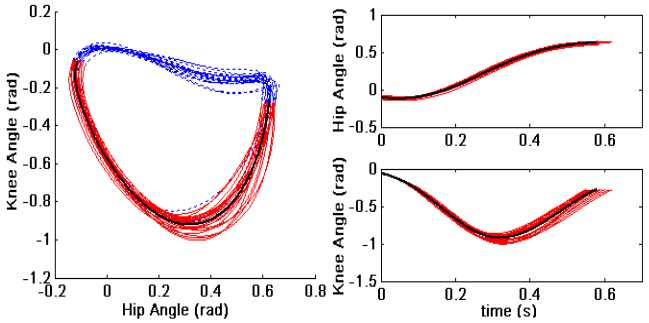

Fig. 7. (a) Hip versus Knee during a trial when treadmill speed was 2 mph. Red lines represent swing phase extracted from full step data represented by red and blue lines combined. Solid black lines represent average swing phase. (b) Hip angle vs time (c) Knee angle vs time.

wearing the device. To estimate the torque, we used a two link human leg model as described in Section II, the filtered joint encoder data and the force-torque data from the sensors. In case 2, we estimated the torque applied by the human when he is not wearing the device but is required to generate the same kinematic pattern as in case 1. If the device was working as intended, on comparison, one would expect to see that the torques required in case 1 are less than that required in case 2.

For the data shown in Fig. 7, the torques required by the human in the two cases are shown in Fig. 8. In these plots, solid red line corresponds to case 1, dotted blue line corresponds to case 2. Ideally, we expect to see the joint torques required by human to be zero in the device (case 1), since the device parameters were found based on the assumption of zero-input from human. However, in Fig. 8(a), we see that the torque required in case 1 is negative for most part of the swing phase. These errors may be due to modeling of the trunk motion, unaccounted compliances of the leg muscles, non-ideal torsion springs, friction in the joints, device and human joint axes mismatch. Observe that during the initial part of the swing phase the magnitude of the torque required in case 1 is more than that of the torque required in case 2, however, it is reduced during the rest of the swing phase. Also, observe that the peak absolute magnitude of case 1 torque ($\approx$ 5 Nm) is much less than that of the case 2 torque ($\approx$ 14.5 Nm) - indicating that the person with less than normal muscle strength might be able to perform this particular gait pattern better with the device than without it. Doing a similar comparison for knee joint torque shows that the peak absolute torque with the device is comparable to the peak absolute torque without it, indicating that the device is not making a big difference for the muscles related to the knee joint.

Figures 9(a),(b) show the difference of the absolute values of the magnitude of torque required in case 2 and case 1 for different treadmill speeds (1 mph - 4 mph). Mathematically, this quantity is $(|\tau_{1_H}| - |\tau_{1_D}|)$ for hip and $(|\tau_{2_H}| - |\tau_{2_D}|)$ for knee. Subscripts 1, 2 stand for hip and knee joints and the subscripts H and D stand for 'human without device' (case 2) and 'human with device' (case 1) respectively. The time scale is normalized over different treadmill speeds to aid a better comparison. In these graphs, more the positive area, the better the effectiveness of the device for that speed. For the hip joint, we see that the curve corresponding to 2 mph treadmill speed has the maximum positive area and for the knee joint, the curve corresponding to 4 mph treadmill speed has the maximum postive area. As noted earlier, for the 2 mph treadmill speed, the knee joint torque has approximately equal positive and negative areas - showing that the device is effective for certain part of the swing phase and ineffective during the rest of the swing phase. Tweaking the stiffness of the torsion springs and their equilibrium configurations might give a desirable performance even at knee joint for this treadmill speed. Among the current trials, if we have to strike a balance between device effectiveness at hip and knee joints then the 4 mph trial seems to give a better performance.

In the graphs shown in Figs. 9(a),(b) the sign of the torques is not reflected adequately. Torque in case 1 may be less in magnitude compared to case 2 but they may have the same sign or opposite sign. These two cases are clearly distinguished in Figures 10(a),(b) where the device effectiveness at different treadmill speeds is compared by preserving the sign but not the magnitude. In these figures, the baseline stands for the device not being effective, a unit step means that the device is effective in magnitude but torques in case 1 and case 2 have opposite signs. A two unit step signifies that the device is effective both in magnitude and the torques have the same sign. Like earlier, even in these graphs, more the area under the graphs, the higher the effectiveness of the device is at that treadmill speed. On comparison, we see that for the hip, the 2.0 mph treadmill speed trial has the maximum area. The 3.0 and 4.0 mph speed trials also have comparable areas. For the knee, the 2.0 mph and 4.0 mph treadmill speed trials have more area than the other trials.

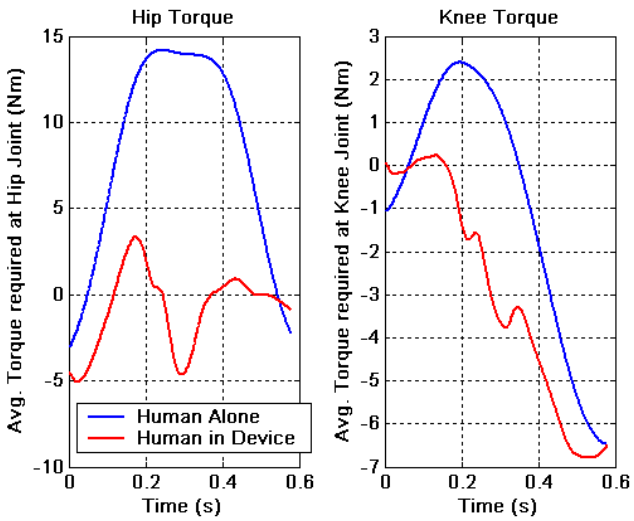

Fig. 8. Torque required to be applied by human at hip when treadmill speed is 2.0 mph

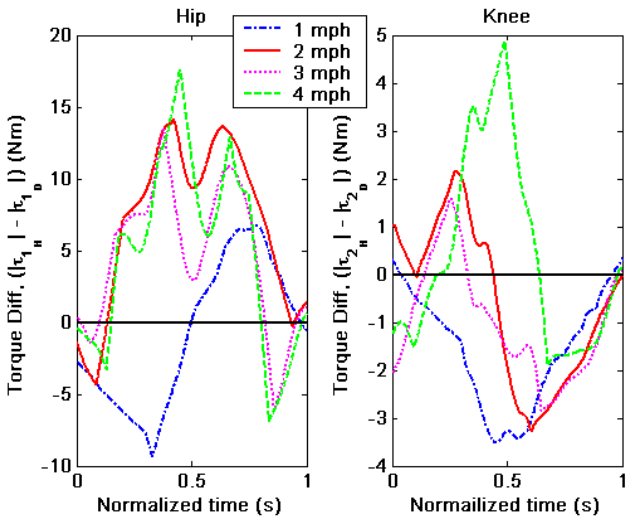

Fig. 9. The difference in torque 'without device' and 'with device' is plotted against time for the hip and knee joints. The treadmill speed is varied from 1.0 mph to 4.5 mph.

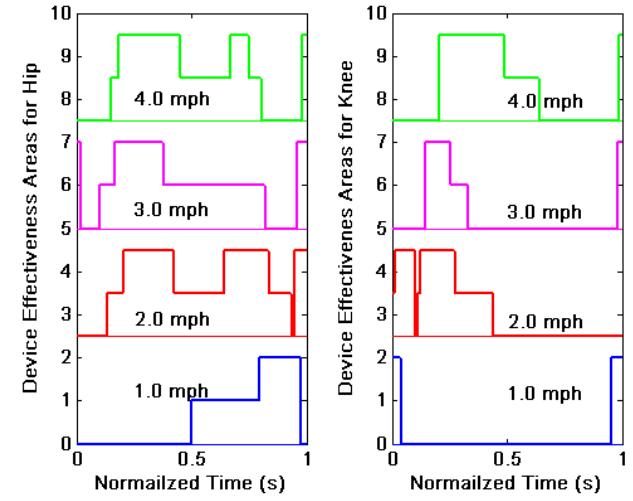

Fig. 10. Device effectiveness areas for different treadmill speeds (a) at Hip joint (b) at Knee joint.

Conclusions

In this paper, we presented a simple passive bilateral exoskeleton for swing assistance of motor incomplete spinal cord injury (iSCI) patients. This exoskeleton is aimed at reducing the physical and financial costs associated with therapist assisted training. The device consists of two segments - thigh and shank with torsion springs at hip and knee joints. Stiffness of the springs and their equilibrium configurations were considered to be the design parameters. We modeled the human leg as a two link leg with thigh and shank segments. Foot was modeled as a point mass and the hip had a prescribed vertical motion. For this model, we wrote the dynamics when the device is strapped onto the leg and performed optimization to find the design parameters. In the simulation, we observed that the device helps the leg during swing phase to obtain ground clearance and go to the desired final configuration with a certain cycle time. We also performed simulations with change in leg mass to observe the robustness of the design to variation of system parameters. We found that the system was robust for upto 50% change in leg mass. We performed multi-step simulations to check the stability of the design over a period of time. From these simulations, we observed that the system remains stable, even when the leg mass was changed by 50%.

An experimental device was made based on the optimization parameters found from simulations. This device was tested on a healthy subject at different treadmill speeds. To show the effectiveness of the device, we compare two different cases. In case 1, we estimated the torque applied by the human when walking with the device. In case 2, we calculated the required torque to perform a similar gait trajectory as that in case 1. On analysis, we found that at 2.0 mph, the device was effective in reducing the maximum torque requirement at hip joint but not so effective at the knee joint. At 4.0 mph, the device seems to show good effectiveness at both hip and knee joints. Certain modeling errors, parameter uncertainity, non-ideal spring behavior, friction in joints and joint axes mismatch might have contributed to the deviation from the results shown in simulation results. But, nevertheless, it promises to help patients with less than normal muscle strength to achieve better gait trajectories. Further tweaking of the torsion spring parameters might help in achieving better device effectiveness even at knee joint.

Acknowledgements

We acknowledge support of NIH through R20 subcontract from Rehabilitation Institute of Chicago and BRP grant. We also acknowledge Vivek Sangwan and for valuable inputs.

References

[1] NSCISC (National Spinal Cord Injury Statistical Center), Birmingham, AL, 2005.

[2] Dobkin B., Apple D., Barbeau H., Basso M., Behrman A., Deforge D., Weight-supported treadmill vs over-ground training for walking after acute incomplete SCI, *Neurology*, vol. 66, no. 4, 2006, pp 484-93.

[3] Colombo G., Joerg M., Schreier R., Dietz V., Treadmill training of paraplegic patients using a robotic orthosis, *J Rehabil Res Dev*, vol. 37, no. 6, 2000, pp 693-700.

[4] Hornby T.G., Zemon D.H., Campbell D., Robotic-assisted, body-weight-supported treadmill training in individuals following motor incomplete spinal cord injury, *Phys Ther*, vol. 85, no. 1, 2005, pp 52-66.

[5] Gottschall J.S., Kram R., Energy cost and muscular activity required for leg swing during walking, *J Appl Physiol*, vol. 99, no. 1, 2005, pp 23-20.

[6] Rahman T., Sample W., Seliktar R., Design and testing of WREX, *The Eighth International Confrence on Rehabilitation Robotics* , Kaist, Daejeon, Korea 2003.

[7] Agrawal S.K., Fattah A., Theory and design of an orthotic device for full or partial gravity-balancing of a human leg during motion, *IEEE Trans Neural Syst Rehabil Eng*, vol. 12, no. 2, 2004, pp 157-65.

[8] Banala S.K., Agrawal S.K., Fattah A., Rudolph K., Scholz J., Gravity balancing leg orthosis and its Performance Evaluation, *IEEE Trans on Robotics*, Vol 22, No. 6, 2006, pp 1228-1239.

[9] Winter D.A., *Biomechanics and Motor Control of Human Movement* , John Wiley & Sons, Inc., 1990, Chapter 3.